View Article Online / Journal Homepage

Dalton Transactions

Accepted Manuscript

Downloaded by Georgetown University Library on 28 November 2012
Published on 27 November 2012 on http://pubs.rsc.org | doi:10.1039/C2DT32167J

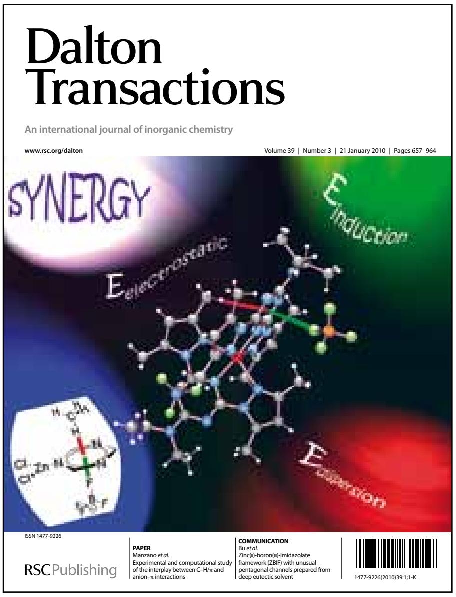

Dalton Transactions

An international journal of inorganic chemistry

www.rsc.org/dalton

Volume 39 | Number 3 | 21 January 2010 | Pages 657–964

ISSN 1477-9226

RSC Publishing

PAPER
Manzano *et al.*
Experimental and computational study of the interplay between C–H/π and anion–π interactions

COMMUNICATION
Bu *et al.*
Zinc(II)-boron(III)-imidazolate framework (ZBF) with unusual pentagonal channels prepared from deep eutectic solvent

This is an *Accepted Manuscript*, which has been through the RSC Publishing peer review process and has been accepted for publication.

Accepted Manuscripts are published online shortly after acceptance, which is prior to technical editing, formatting and proof reading. This free service from RSC Publishing allows authors to make their results available to the community, in citable form, before publication of the edited article. This *Accepted Manuscript* will be replaced by the edited and formatted *Advance Article* as soon as this is available.

To cite this manuscript please use its permanent Digital Object Identifier (DOI®), which is identical for all formats of publication.

More information about *Accepted Manuscripts* can be found in the **Information for Authors**.

Please note that technical editing may introduce minor changes to the text and/or graphics contained in the manuscript submitted by the author(s) which may alter content, and that the standard **Terms & Conditions** and the **ethical guidelines** that apply to the journal are still applicable. In no event shall the RSC be held responsible for any errors or omissions in these *Accepted Manuscript* manuscripts or any consequences arising from the use of any information contained in them.

RSC Publishing

www.rsc.org/dalton

Registered Charity Number 207890

Dalton Transactions

Dynamic Article Links ▶

View Article Online

Cite this: DOI: 10.1039/c0xx00000x

www.rsc.org/xxxxxx

PAPER

Copper(I) complexes of 1,10-phenanthroline and heterocyclic thioamides: an experimental and theoretical (DFT) investigation of the photophysical characteristics

Ioannis Papazoglou,[a] Philip J. Cox,[b] Anastasios G. Papadopoulos,[c] Michael P. Sigalas[c] and Paraskevas Aslanidis[a]*

Received (in XXX, XXX) Xth XXXXXXXXX 20XX, Accepted Xth XXXXXXXXX 20XX
DOI: 10.1039/b000000x

A series of luminescent mixed ligand complexes of copper(I) halides with 1,10-phenanthroline and the heterocyclic thioamides pyridine-2(1H)-thione (py2SH), pyrimidine-2(1H)-thione (pymtH), 4,6-dimethylpyrimidine-2(1H)-thione (dmpymtH), 1,4,5,6-tetrahydropyrimi-dine-2-thione (thpymtH), 1,3-imidazolidine-2-thione (imtH$_2$) and 4,5-diphenyl-2-oxazolethiol (dpoxtH) have been synthesized and characterized. The molecular structures of two representative compounds have been established by single-crystal X-ray diffraction. The mononuclear complexes feature the metal in a distorted tetrahedral environment surrounded by the two N atoms of the chelating 1,10-phenanthroline, the thione-S atom of the thioamide, and the halogen atom. The molecular structure, the electronic and photophysical properties and the energetics of the metal-ligand interactions for [CuI(phen)(py2SH)] have been studied by means of density functional calculations.

1. Introduction

Much attention has been paid in the past two decades to emissive coordination compounds of many transition metals in view of their applications as dopants to increase the electroluminescence efficiency of organic light emitting diodes,[1–3] as sensitizers in solar-energy conversion,[4,5] as components for luminescent-based chemical sensors,[6–9] in display devices[10,11] and as photocatalysts. In this respect, first row transition metal complexes are particularly attractive, being considered as inexpensive, less toxic and more easily available potential alternatives to the currently used third-row noble metal complexes. Among the emissive tetrahedral copper(I) complexes investigated so far, the most promising class involve polypyridine- and phenanthroline-type ligands,[12,13] often combined with other rigid chelating ligands such as diphosphanes.[14–17] One of the most interesting findings of the earlier investigations on copper(I) bis-phenanthroline complexes was the fact that their spectral characteristics were related to the distortions from the tetrahedral geometry induced by the substituents on the chelating ligands. In fact, it could be shown than [Cu(I)(2,9-dimethyl-1,10-phenanthroline)$_2$]$^+$ exhibits photoluminescence in dichloromethane but not in methanol or acetonitrile, whereas solutions of [Cu(I)(1,10-phenanthroline)$_2$]$^+$ are not emissive.[18–20] This was attributed to a distortion in the MLCT excited state due to a change of the formal oxidation state from Cu(I) to Cu(II), generating a more flattened geometry around the formed d^9 metal ion, which offers a further coordination site for nucleophilic attack by species such as solvent molecules. This flattening distortion, responsible for the quenching of the excited state, is efficiently prevented by the presence of bending substituents in the 2,9-positions of the phenanthroline ligand. Subsequent work involved the development of mixed-ligand copper(I) complexes which possess, in addition to their ability to overcome solvent-induced exciplex quenching, enhanced emission characteristics (intensity, lifetime, and quantum yield). As well as the use of sterically hindered phenanthroline ligands, electronic factors induced by suitable spectator co-ligands might also influence the oxidative instability of these complexes.

It is well known that the coordination chemistry of the soft acid copper(I) is largely based upon coordination to ligands containing soft donor atoms such as P or S. In this sense, copper(I) complexes containing heterocyclic thioamides have received a great deal of attention during the past few decades,[21–24] whereby plenty of interesting structures, in which the neutral thioamide molecules were generally found to bind the metal through the exocyclic sulfur atom, were obtained. Exploring the photochemistry of such mixed-ligand copper(I) complexes incorporating neutral heterocyclic thiones or thiolates in the coordination sphere we recently reported on two series of Cu(I) compounds formulated as [Cu(κ^3-triphos)(thiolate)][25] and [CuX(DPEphos)(thione)][26], respectively. Noticeably, the emission energy of these complexes proved to be tunable by modifying the ligands as well as introducing electron-donating or -accepting substituents to the heterocyclic rings. In an attempt to elucidate whether and how far the heterocyclic thione ligands could affect the photophysical properties of mixed-ligand copper(I) phenanthroline complexes and to test the expectation that oxidative instability of the complexes can be suppressed due to the pronounced tendency of thioamides to stabilize copper in its lower oxidation state, we present herein a series of novel complexes, which turn out to exhibit quite interesting luminescent properties.

Further, density functional calculations for the complex [CuI(phen)(py2SH)] are used to interpret the relationship between structure electronic and photophysical properties, as well as to explore the energetics of the metal-ligand interactions.

2. Experimental Section

2.1. Materials and instrumentation

All air sensitive manipulations were performed under argon using standard Schlenk techniques. Commercially available copper (I) halides and 1,10-phenanthroline were used as received, whereas the heterocyclic thioamides pyridine-2(1H)-thione (py2SH), pyrimidine-2(1H)-thione (pymtH), 4,6-dimethylpyrimidine-2(1H)-thione (dmpymtH), 1,4,5,6-tetrahydropyrimidine-2-thione (thpymtH), 1,3-imidazolidine-2-thione ($imtH_2$), 4,5-diphenyl-2-oxazolethiol (dpoxtH) and 1,3-diphenyl-2-thiobarbituric acid (dptba) (Scheme 1) were recrystallized from hot ethanol. All the solvents were purified by respective suitable methods and allowed to stand over molecular sieves. Infra-red spectra in the region of 4000–200 cm^{-1} were obtained in KBr discs with a Nicolet FT-IR 6700 spectrophotometer. Electronic absorption spectra in dichloromethane solutions were measured with a Shimadzu 160A spectrophotometer, while a Hitachi F-7000 fluorescence spectrophotometer was used to obtain the excitation and emission spectra. Melting points were measured in open tubes with a STUART scientific instrument and are uncorrected.

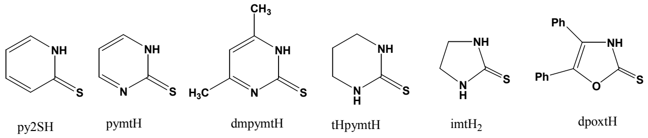

Scheme 1 The heterocyclic thioamides used as ligands with their abbreviations

2.2. Crystal structure determination

Single crystals of **3** suitable for crystal structure analysis were obtained from an acetonitrile/methanol mixture of the complex at 5°C under argon, whereas crystals of **7** were grown in a dichloromethane/acetonitrile solution at room temperature. X-ray diffraction data were collected on a Rigaku Saturn 724+ diffractometer by the NCS[27] using *CrystalClear-SM Expert*[28] for cell refinement, data collection and data reduction. The structure was solved with *SHELXS97*[29] and refined with *SHELXL97*. The program used for Molecular graphics was *PLATON*.[30] Tables for publication were prepared with *SHELXS97* and *WINGX*.[31]

2.3. Computational details

DFT and TD-DFT calculations of CuI(phen)(py2SH) (compound **3**) were carried out with Gaussian 03W[32] software package under the PCM[33-35] algorithm implemented in it. Geometry optimizations were carried out in ground state (S_0) and in triplet state (T_1). A frequency calculation after each geometry optimization ensured that the calculated structures are real minima in the potential energy surface of the molecules. The calculations were carried out not only in gas phase, but in dichloromethane solution as well using the PCM model. The PBE1PBE[36,37]functional of Perdew, Burke and Ernzerhof was used in combination with the 6-311++G(d,p)[38–42] basis set for the elements C, N, H, S and the SDD effective core potentials and basis set for the elements Cu and I. Test calculations show that PBE1PBE functional give better results than B3LYP in calculating the molecular structure. Furthermore, PBE1PBE gave better results for spectrum analysis than BP86. Thus, the PBE1PBE functional has been chosen both for geometry optimizations and for calculating the spectra. Visualization of the MOs of interest was done with GaussView 4.1.

2.4. Synthesis

To a 40 ml round-bottom flask flushed with argon and equipped with a stirrer bar was added 15 ml of degased acetonitrile and 0.5 mmol of copper halide (49.5 mg for CuCl, 71.7 mg for CuBr or 95.2 mg for CuI) and the mixture was stirred at 50 °C under a continuous argon stream. To the resulting clear solution, a 10 ml degassed methanol solution containing 90 mg (0.5 mmol) 1,10-phenanthroline and 0.5 mmol of the respective thioamide was then added, whereupon the colour of the solution immediately changed to red. The reaction mixture was stirred for 5 min and then filtered off and collected into a Schlenk flask which was capped and stored at 5 °C for 24 h, whereupon dark red crystals deposited which were collected by filtration and dried in vacuo.

Alternative procedure: To a Schlenk flask flushed with argon and equipped with a stirrer bar was added 10 ml of degased acetonitrile and 0.25 mmol of copper halide (24.7 mg for CuCl, 35.8 mg for CuBr or 47.6 mg for CuI) and the mixture was stirred at 50 °C under a continuous argon stream until a clear solution resulted. After cooling to room temperature, 45 mg (0.25 mmol) 1,10-phenanthroline and 0.25 mmol of the respective thioamide, dissolved in a minimum amount of ~3 ml degassed dichloromethane was added, whereupon the microcrystalline product was deposited within minutes.

2.4.1. [CuCl(phen)(py2SH)] (1). Red crystals (92 mg, 47 %), m.p. 195 °C; Anal. Calc. for $C_{17}H_{13}CuClN_3S$: C, 52.30; H, 3.36; N, 10.76. Found: C, 52.16; H, 3.19; N, 10.45 %. IR (cm^{-1}): 3151w, 3044w, 2952w, 2878m, 1603s, 1576vs, 1506s, 1418s, 1367s, 1131vs, 996s, 843vs, 751vs, 723vs, 486m, 449s; UV-Vis (λ_{max}, log ε): 234 (4.80), 263 (5.32), 300 (3.37), 429 (3.03).

2.4.2. [CuBr(phen)(py2SH)] (2). Red crystals (111 mg, 51 %), m.p. 203 °C; Anal. Calc. for $C_{17}H_{13}CuBrN_3S$: C, 46.95; H, 3.01; N, 9.66. Found: C, 46.23; H, 2.91; N, 9.45 %. IR (cm^{-1}): 3142w, 3040m, 2957m, 2855m, 1603s, 1571vs, 1502s, 1409s, 1362s, 1131vs, 992s, 843vs, 746vs, 727vs, 486s, 449s; UV-Vis (λ_{max}, log ε): 232 (4.78), 270 (5.32), 396 (3.81), 435 (3.66).

2.4.3. [CuI(phen)(py2SH)] (3). Red crystals (108 mg, 45 %), m.p. 208 °C; Anal. Calc. for $C_{17}H_{13}CuIN_3S$: C, 42.38; H, 2.72; N, 8.72. Found: C, 42.31; H, 2.63; N, 8.73 %. IR (cm^{-1}): 3138w, 3045m, 2976m, 2910s, 1604s, 1566vs, 1502s, 1418s, 1362s, 1219m,1131vs, 992s, 839vs, 741vs, 727vs, 486s, 449s; UV-Vis (λ_{max}, log ε): 232 (4.83), 270 (5.10), 366 (4.93), 422sh (3.52).

2.4.4. [CuCl(phen)(pymtH)] (4). Red microcrystals (86 mg, 44 %), m.p. 200 °C; Anal. Calc. for $C_{16}H_{12}CuClN_4S$: C, 49.10; H, 3.09; N, 14.31. Found: C, 48.98; H, 3.15; N, 14.22 %. IR (cm^{-1}): 3051m, 2922m, 1603s, 1563vs, 1514s, 1425vs, 1376vs, 1331s, 1176vs, 975s, 850vs, 771m, 726vs, 46ms; UV-Vis (λ_{max}, log ε): 231 (4.77), 271 (5.05), 404 (3.55); UV-Vis (λ_{max}, log ε): 234 (4.31), 261 (4.23), 290 (3.98), 403 (2.85).

2.4.5. [CuCl(phen)(pymtH)] (5). Red microcrystals (85 mg, 39 %), m.p. 206 °C; Anal. Calc. for $C_{16}H_{12}CuBrN_4S$: C, 44.10; H, 2.77; N, 12.85. Found: C, 43.92; H, 2.58; N, 12.82 %. IR (cm^{-1}): 3133w, 3054m, 2985m, 1594vs, 1557vs, 1474s, 1418s, 1316vs, 1214s, 1172vs, 973vs, 871m, 783s, 737s, 454s; UV-Vis (λ_{max}, log ε): 231 (4.77), 271 (5.05), 317sh (3.81), 404 (3.55).

2.4.6. [CuI(phen)(pymtH)] (6). Red powder (113 mg, 47 %), m.p. 214 °C; Anal. Calc. for $C_{16}H_{12}CuIN_4S$: C, 39.80; H, 2.50; N, 11.60. Found: C, 38.98; H, 2.68; N, 11.24 %. IR (cm^{-1}): 3093m, 3050m, 3010m, 2918m, 2855m, 1599s, 1556vs, 1467s, 1421vs, 1371s, 1211m, 1197m, 1173vs, 1137m, 1045m, 979s, 840vs, 762s, 725vs, 470m; UV-Vis (λ_{max}, log ε): 231 (4.80), 271 (5.12), 325sh (3.77), 410 (3.50).

2.4.7. [CuCl(phen)(dmpymtH)] (7). Red crystals (84 mg, 40 %), m.p. 208 °C; Anal. Calc. for $C_{18}H_{16}CuClN_4S$: C, 51.55; H, 3.85; N, 13.36. Found: C, 50.91; H, 3.22; N, 13.28 %. IR (cm^{-1}): 3050m, 2897m, 1613vs, 1562vs, 1423s, 1233vs, 1182s, 982s, 843vs, 723vs, 460m; UV-Vis (λ_{max}, log ε): 231 (4.85), 271 (5.23), 285sh (4.98), 419 (3.32).

2.4.8. [CuBr(phen)(dmpymtH)] (8). Red microcrystals (97 mg, 42 %), m.p. 218 °C; Anal. Calc. for $C_{18}H_{16}CuBrN_4S$: C, 46.61; H, 3.48; N, 12.08. Found: C, 46.58; H, 3.42; N, 11.98 %. IR (cm^{-1}): 3050m, 2915m, 2850m, 1604vs, 1557vs, 1469m, 1423s, 1372s, 1325s, 1210m, 1172vs, 1042m, 978s, 843s, 769m, 723s, 460m; UV-Vis (λ_{max}, log ε): 233 (3.68), 275 (4.58), 295sh (3.08) 414 (3.33).

2.4.9. [CuI(phen)(dmpymtH)] (9). Red crystals (97 mg, 38 %), m.p. 228 °C; Anal. Calc. for $C_{18}H_{16}CuIN_4S$: C, 42.32; H, 3.16; N, 10.97. Found: C, 41.97; H, 3.17; N, 10.86 %. IR (cm^{-1}): 3040m, 2952m, 1608vs, 1557vs, 1506m, 1413s, 1228vs, 1186vs, 9828s, 843vs, 817s, 767m, 727vs, 460m; UV-Vis (λ_{max}, log ε): 229 (4.76), 269 (4.78), 290sh (3.28), 412 (3.70).

2.4.10. [CuCl(phen)(tHpymtH)] (10). Red powder (71 mg, 36 %), m.p. 270 °C; Anal. Calc. for $C_{16}H_{16}CuClN_4S$: C, 48.60; H, 4.08; N, 14.17. Found: C, 48.45; H, 3.95; N, 14.09 IR (cm^{-1}): 3179m, 3114m, 2985m, 1619m, 1566vs, 1506s, 1423s, 1366s, 1214vs, 1141m, 843vs, 767m, 727vs, 635m; UV-Vis (λ_{max}, log ε): 234 (4.35), 256 (4.25), 321 (3.46), 435 (3.04).

2.4.11. [CuBr(phen)(tHpymtH)] (11). Red powder (88 mg, 40 %), m.p. 274 °C; Anal. Calc. for $C_{16}H_{16}CuBrN_4S$: C, 43.69; H, 3.66; N, 12.74. Found: C, 43.52; H, 3.55; N, 12.69 %. IR (cm^{-1}): 3179m, 3118m, 2965m, 1621m, 1575vs, 1566vs, 1505s, 1422s, 1371s, 1320s, 1209vs, 1134m, 843vs, 727vs, 635s, 565m; UV-Vis (λ_{max}, log ε): 237 (5.25), 269 (5.24), 326 (5.08), 435 (2.99).

2.4.12. [CuI(phen)(tHpymtH)] (12). Red crystals (90 mg, 37 %), m.p. 279 °C; Anal. Calc. for $C_{16}H_{16}CuIN_4S$: C, 39.47; H, 3.31; N, 11.51. Found: C, 39.11; H, 2.88; N, 10.65 %. IR (cm^{-1}): 3193s, 3040m, 2957m, 1617m, 1576vs, 1548vs, 1506s, 1418vs, 1372m, 1321s, 1200vs, 945m, 839vs, 723vs, 630m, 467s; UV-Vis (λ_{max}, log ε): 234 (4.94), 267 (5.24), 3.26 (5.36), 437 (2.91).

2.4.13. [CuCl(phen)(imtH$_2$)] (13). Red powder (63 mg, 33 %), m.p. 248 °C; Anal. Calc. for $C_{15}H_{14}CuClN_4S$: C, 47.24; H, 3.70; N, 14.69. Found: C, 47.23; H, 3.71; N, 14.63 %. IR (cm^{-1}): 3263s, 3115s, 3050m, 2897m, 1616m, 1543vs, 1515vs, 1486s, 1422vs, 1321s, 1284s, 1210vs, 1135m, 1033m, 839vs, 727vs, 579s, 500s, 419m; UV-Vis (λ_{max}, log ε): 229 (4.59), 270 (4.95), 297 (3.43), 426 (2.98).

2.4.14. [CuBr(phen)(imtH$_2$)] (14). Red powder (68 mg, 32 %), m.p. 254 °C; Anal. Calc. for $C_{15}H_{14}CuBrN_4S$: C, 42.31; H, 3.31; N, 13.16. Found: C, 42.33; H, 3.30; N, 13.08 %. IR (cm^{-1}): 3263s, 3156s, 3045m, 2892m, 1619m, 1539vs, 1518vs, 1489s, 1418vs, 1321s, 1284s, 1205vs, 1131m, 839vs, 727vs, 700s, 574s, 496s; UV-Vis (λ_{max}, log ε): 233 (4.59), 272 (5.05), 295 (4.79), 434 (2.99).

Table 1 Crystal Data and Structure Refinement for [CuI(phen)(py2SH)] (**3**) and [CuCl(phen)(dmpymtH)]$\cdot$$CH_2Cl_2$ (**7**)

	3	**7**
Molecular formula	$C_{17}H_{13}CuIN_3S$	$[(C_{18}H_{16}ClCuN_4S)(CH_2Cl_2)]$
Formula weight	481.80	504.33
Temperature	100(2) K	100(2) K
Wavelength	0.71073 Å	0.71073 Å
Crystal system	Triclinic	Monoclinic
Space group	P$\bar{1}$	Cc
Unit cell dimensions	a = 7.9266(11) Å b = 9.2093(16) Å c = 13.107(3) Å α= 85.396(18)° β= 72.771(13)° γ = 67.540(14)°	a = 25.97(2) Å b = 11.156(8) Å c = 16.699(13) Å α= 90° β= 118.877(14)° γ = 90°
Volume	844.0(3) $Å^3$	4236(6) $Å^3$
Z	2	8
Density (calculated)	1.896 Mg/m^3	1.581 Mg/m^3
Absorption coefficient	3.248 mm^{-1}	1.521 mm^{-1}
F(000)	468	2048
Crystal size	0.20 x 0.06 x 0.02 mm^3	0.10 x 0.06 x 0.02 mm^3
Theta range for data collection	2.85 to 27.50°	1.65 to 31.27°
Index ranges	-10<=h<=10 -11<=k<=9 -17<=l<=16	-36<=h<=35 -16<=k<=16 -20<=l<=23
Reflections collected	7844	31791
Independent reflections	3805 [R(int) = 0.0184]	10710 [R(int) = 0.0698]
Completeness to theta = 27.50°	98.0 % (theta = 27.50°)	92.9 % (theta = 31.27°)
Max. and min. transmission	0.9379 and 0.5628	1.00 and 0.77
Refinement method	Full-matrix least-squares on F^2	Full-matrix least-squares on F^2
Data / restraints / parameters	3805 / 0 / 208	10710 / 2 / 510
Goodness-of-fit on F^2	0.977	1.115
Final R indices [I>2sigma(I)]	R1 = 0.0173, wR2 = 0.0408	R1 = 0.0775, wR2 = 0.1741
R indices (all data)	R1 = 0.0201, wR2 = 0.0412	R1 = 0.0930, wR2 = 0.1861
Final weighting scheme	calc $w=1/\sigma^2[(Fo^2)+(0.0183 P)^2+ 0.0000P]$, where $P=(Fo^2+2Fc^2)/3$	calc $w=1/\sigma^2[(Fo^2)+(0.0694 P)^2+ 8.9316P]$, where $P=(Fo^2+2Fc^2)/3$
Absolute structure parameter		0.0(2)
Largest diff. peak and hole	0.656 and -0.426 e.$Å^{-3}$	0.942 and -0.861 e.$Å^{-3}$

2.4.15. [CuI(phen)(imtH$_2$)] (15). Red powder (92 mg, 39 %), m.p. 259 °C; Anal. Calc. for $C_{15}H_{14}CuIN_4S$: C, 38.10; H, 2.98; N, 11.85. Found: C, 38.07; H, 2.97; N, 11.42 %. IR (cm^{-1}): 3217s, 3140s, 2878m, 1622m, 1502vs, 1423vs, 1325s, 1274s, 1191s, 839vs, 765m, 727vs, 666m, 602m, 489m; UV-Vis (λ_{max}, log ε): 232 (4.79), 271 (5.26), 288 (4.23), 422 (3.13).

2.4.16. [CuCl(phen)(dpoxtH)] (16). Red powder (101 mg, 38 %), m.p. 218 °C; Anal. Calc. for $C_{27}H_{19}CuClN_3OS$: C, 60.90; H, 3.60; N, 7.89. Found: C, 60.43; H, 3.12; N, 7.85 %. IR (cm^{-1}): 3054m, 2925w, 1507s, 1492vs, 1425vs, 1182vs, 1021m, 955s, 848s, 764vs, 727s, 695vs, 598m, 556s, 520m; UV-Vis (λ_{max}, log ε): 230 (4.76), 268 (5.06), 322 (3.39), 417 (3.04).

2.4.17. [CuBr(phen)(dpoxtH)] (17). Red powder (68 mg, 32 %), m.p. 223 °C; Anal. Calc. for $C_{27}H_{19}CuBrN_3OS$: C, 56.21; H, 3.32; N, 7.28. Found: C, 55.82; H, 3.32; N, 7.22 %. IR (cm^{-1}): 3023m, 2860m, 1505s, 1492vs, 1423vs, 1182vs, 1027m, 964s, 848vs, 760vs, 695vs, 587m, 556s, 517m; UV-Vis (λ_{max}, log ε): 233 (4.74), 270 (5.19), 317 (4.39), 403 (3.06).

2.4.18. [CuI(phen)(dpoxtH)] (18). Red powder (106 mg, 34 %), m.p. 228 °C; Anal. Calc. for $C_{27}H_{19}CuIN_3OS$: C, 51.97; H, 3.07; N, 6.73. Found: C, 51.42; H, 2.92; N, 7.08 %. IR (cm^{-1}): 3028m, 2906m, 1505s, 1492vs, 1418vs, 1177vs, 1021m, 964s, 843vs, 760vs, 727vs, 690vs, 583m, 556s, 517m; UV-Vis (λ_{max}, log ε): 232 (4.97), 272 (5.35), 330 (4.26), 407 (3.30).

3. Results and discussion

3.1. Synthesis

Compounds **1-18** are accessible via the direct treatment of copper(I) halides with equivalent amounts of 1,10-phenanthroline and the corresponding heterocyclic thioamide under mild conditions. The complexes formed immediately after mixing the solutions of the components, which becomes apparent from the dark red colour of the reaction mixture, are quite unstable in solution. In fact, their solutions undergo gradual re-colouring from red to green, which indicates oxidation of copper(I) to copper(II). Thus, the choice of the proper reaction medium in order to gain control over the speed of the subsequent crystal deposition, was crucial for the successful isolation of the desired compounds in pure form. In this respect, rapid and very efficient precipitation was obtained in acetonitrile/ dichloromethane solutions, whereas the acetonitrile/methanol mixture, though less suitable for the more sensitive derivatives, proved to be an appropriate medium for better crystal growth. Interestingly, the above oxidation process was also found to depend on the type of the thioamide used. Indeed, in some cases solutions tended to undergo decomposition within minutes, whereas in the specific case of tHpymtH the corresponding complexes (compounds **10-12**) were less sensitive to oxidation and their solutions remained stable for relative long time.

3.2. Spectroscopy

In the infrared spectra of compounds **1-18**, recorded in the range 4000–250 cm^{-1}, the two very strong phenanthroline bands at ~840 and ~740 cm^{-1} display a red shift of about 15 cm^{-1} upon coordination, whereas a strong band at ~620 cm^{-1} appears blue-shifted by about 10 cm^{-1}. Further multiple strong bands in the range 1590–1430 cm^{-1} attributable to the phenathroline molecule remain practically unshifted upon coordination. In addition, the spectra of all compounds contain the expected four characteristic “thioamide bands”, with shifts due to coordination indicative of an exclusive S-coordination mode.

The electronic absorption spectra of all compounds are dominated by two intense UV bands in the range ~230 and ~270 nm. Exact assignment of these bands is difficult since both the thiones ligands and phenanthroline strongly absorpts in these two regions. A third broad band of lower intensity in the 300-360 nm region can be ascribed to thione originating intraligand transitions, which may possess partial charge transfer CT character. The lowest-energy band of the absorption spectra for the complexes consisting of a band with maxima in the 400–435 nm near UV region have been assigned to metal to ligand charge transfer (MLCT) bands of the phenanthroline ligand.[43–44]

3.3. X-ray structural analysis

The X-ray crystal structures of [CuI(phen)(py2SH)] (**3**) and [CuCl(phen)(dmpymtH)]·CH_2Cl_2 (**7**) (details of crystal and structure refinement are shown in Table 1) corroborate the spectroscopic results discussed above. Main bond lengths and angles are listed in Tables 2 and 3, whereas plots for the two molecules showing the atom numbering appear in Figures 1 and 2 respectively. The crystals of 7 were twinned and the extent of the available data was limited to 93% of that normally expected. The alternate space group, C2/c, was considered as a pseudo centre of symmetry is present but refinement in this space group was unstable. There are two molecules in the asymmetric unit of **7**, with small geometrical differences between them; table 3 contains selected bond lengths and angles only for one of these molecules.

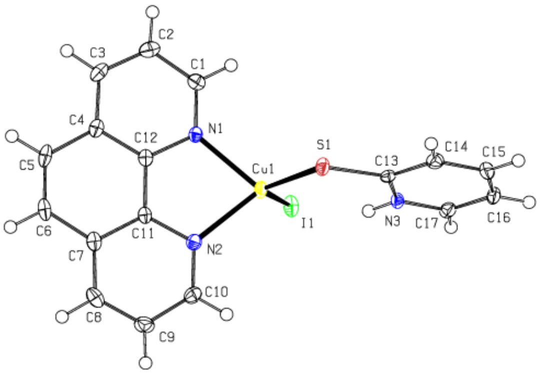

Fig. 1 A molecular plot of [CuI(phen)(py2SH)] (**3**)

Table 2 Selected bond lengths [Å] and angles [°] for **3**

Cu(1)–I(1)	2.6216(5)	Cu(1)–N(1)	2.0836(16)
Cu(1)–N(2)	2.1177(15)	Cu(1)–S(1)	2.2343(6)
S(1)–C(13)	1.7081(19)		
N(1)–Cu(1)–N(2)	79.74(6)	N(1)–Cu(1)–S(1)	112.14(4)
N(2)–Cu(1)–S(1)	122.12(5)	N(1)–Cu(1)–I(1)	106.12(4)
N(2)–Cu(1)–I(1)	108.18(4)	S(1)–Cu(1)–I(1)	120.331(19)
C(13)–S(1)–Cu(1)	111.35(7)		
Hydrogen bridge			
N(3)–H(3)	0.8800	N(3) ··· I(1)	3.4440(16)
NH(3)–I(1)	2.6100	I(1)···H(3)–N(3)	158.3°

The four-coordinate monomers reveal a copper coordination sphere consisting of two N atoms of the phenanthroline molecule, the S atoms from two corresponding thione unit and the halogen atom. The angular deviations from the ideal tetrahedral value are remarkable but not at all unexpected, at least regarding the acute N–Cu–N angle which is 79.74(6)^o in **3** and 80.2(2)^o in **7**, restricted by the narrow bite angle of the rigid phenanthroline unit. This angle is very close to that of 79.93(10)^o observed in [CuI(phen)(PPh$_3$)],[45] or 80.6(1)^o found in [Cu$_2$(μ-I)$_2$(phen)$_2$],[46] and within the range of values found in other related complexes.[47–49]

The CuNCCN framework in **3** shows the formation of an almost planar five-membered chelate ring, whereas in the structure of **7,** in one of the two molecules the Cu1 atom is displaced from a mean plane through the N1,N2,C1-C12 atoms by 0.25A, whereas in the other molecule the Cu2 atom is almost co-planar, i.e., it is only displaced by 0.05A from the N5,N6,C19-C30 plane.

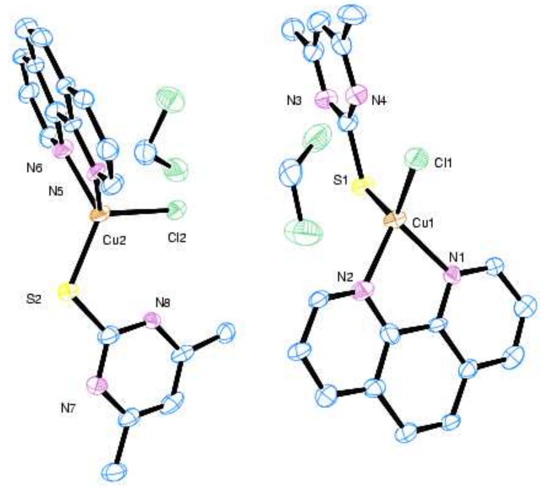

Fig. 2 The asymmetric unit of [CuCl(phen)(dmpymtH)].[CH$_2$Cl$_2$] (**7**)

Table 3 Selected bond lengths [Å] and angles [°] for **7**

Cu(1)–Cl(1)	2.307(2)	Cu(1)–N(1)	2.112(6)
Cu(1)–N(2)	2.136(7)	Cu(1)–S(1)	2.241(2)
S(1)–C(13)	1.732(7)		
N(1)–Cu(1)–N(2)	80.2(2)	N(1)–Cu(1)–S(1)	105.93(17)
N(2)–Cu(1)–S(1)	122.64(18)	N(1)–Cu(1)–Cl(1)	119.01(17)
N(2)–Cu(1)–Cl(1)	107.82(18)	S(1)–Cu(1)–Cl(1)	116.59(9)
C(13)–S(1)–Cu(1)	111.3(2)		
Hydrogen bridge			
N(4)–H(4)	0.8800	N(4)···Cl(1)	3.1470(6)
NH(4)–Cl(1)	2.2700	Cl(1)···H(4)–N(4)	174.3^o

The Cu–N(1) and Cu–N(2) bond distances of 2.084 and 2.118 Å in **3**, slightly shorter than the corresponding bond distances in **7** are in good agreement with the lengths in analogous compounds.

Likewise the Cu–I bond length in **3** and the Cu–Cl bond length in **7** are comparable to those reported for other tetrahedrally coordinated copper(I) complexes with terminal iodine and chlorine donors respectively.[50-52]

In **3** the shortest intermolecular π...π stacking interaction is 3.513(1) Å between N3-C13-C14-C15-C16-C17 rings separated by the symmetry operation 1-x,1-y,-z. There is also a H... π interaction of 2.58 Å between C14-H14 and the centre of the N2-C10-C9-C8-C7-C11 ring when the coordinates of the ring atoms are displaced by x,1+y,z.

In 7 the shortest intermolecular π...π stacking interaction is 3.423(5)Å between rings N7-C31-N8-C34-C33-C32 and N3-C13-N4-C16-C15-C14 when coordinates of the latter ring atoms are transformed by 0.5+x,0.5-y,-0.5+z. The only H... π interaction is between C17-H17b and the centre of ring N1-C1-C2-C3-C4-C12 when the coordinates of the ring atoms are transformed by x,-y,0.5+z..

3.4. Luminescence

The RT luminescence spectra of the complexes in degassed CH$_2$Cl$_2$ solutions have been studied. The excitation and emission spectrum of a representative compound, [CuCl(phen)(dmpymtH)], is shown in Figure 3 while excitation and emission data of the complexes under investigation are summarized in Table 4.

Table 4 Room temperature excitation and emission maxima of the complexes in 10^{-4} M CH$_2$Cl$_2$ solution

Compound	λ_{exc} [nm]	λ_{em} [nm]
[CuCl(phen)(py2SH)]	387	481
[CuBr(phen)(py2SH)]	350	541
[CuI(phen)(py2SH)]	340	527
[CuCl(phen)(pymtH)]	346, 376	430, 647
[CuBr(phen)(pymtH)]	375	650
[CuI(phen)(pymtH)]	386, 430	540, 648
[CuCl(phen)(dmpymtH)]	376	511
[CuBr(phen)(dmpymtH)]	353	484
[CuI(phen)(dmpymtH)]	372	513
[CuCl(phen)(tHpymtH)]	364	537
[CuBr(phen)(tHpymtH)]	383	490
[CuI(phen)(tHpymtH)]	390	525
[CuCl(phen)(imdztH)	311	533
[CuBr(phen)(imdztH)	385	540
[CuI(phen)(imdztH)	309	535
[CuCl(phen)(dpoxtH)]	364	440
[CuBr(phen)(dpoxtH)]	363	438
[CuI(phen)(dpoxtH)]	353	442

After excitation at 376 nm, the RT emission spectrum of [CuCl(phen)(dmpymtH)] consists of a broad band with maximum at 511 nm, clearly red-shifted by 74 and 102 nm when compared with the emission maxima of both the free ligands dmpymtH and phenanthroline respectively. This result may be considered as evidence for participation of an S→Cu charge transfer in the emissive excited state.[53] In a similar manner, the emission spectra of the other complexes are simple, with bands in the 430–650 nm window, with the $\lambda_{max(em)}$ values strongly depending on the nature of the thione present, whereby the higher energy emissions are registered for the derivatives containing 4,5-biphenyl-2-oxazolino-2-thione (dpoxtH). These variations of the emission bands are obviously associated with the electronic characteristics of the thione ligands which determine the strength of the Cu–S bond. Indeed, recent studies on complexes of type CuXL (L = heteroaromatic ligand) showed that the energy of the emitting excited state can be modulated by modifying the electrophilic properties of L,[54] however precise statements can not be made on the basis of the compounds under investigation.

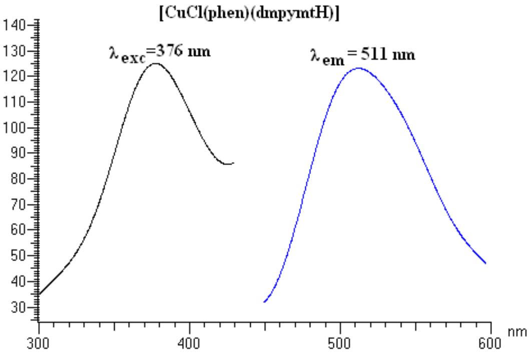

Fig. 3 Room temperature excitation (a) and emission (b) spectrum of [CuCl(phen)(dmpymtH)] in CH_2Cl_2 solution

According to the above observations, the lowest energy emissive excited state can be assigned to MLCT transitions of type Cu^I → thione, since is very likely for the d^{10} ion to express strong tendency for charge transfer of this type. Nothing certainly can be said with regard to the role of the halogen present in each case, though it is very likely for the halogen to participate, to some extent, in the emissive excited states with charge transfer processes of type X→ Cu^I or X→thione.

An additional possibility for low-energy excitation in the complexes under investigation offers the Cu^I → phenanthroline charge transfer. However, excitation in the region 400-430 nm, where the lowest energy band, attributable to this MLCT transition in the UV-vis spectra of the complexes lies, unexpectedly does not cause any emission, except for the three pymtH derivatives, whose spectra contain two emission bands at two different regions, ~ 440 and ~ 650 nm, produced by two different excitations at ~ 340 and ~ 380 nm, respectively. The emissive states in these later compounds could be of mixed MLCT character including both the phenantroline and the thione ligand.

3.5. Computational studies

The skeletal structure of CuI(phen)(py2SH)] is shown in Scheme 2. The molecular structure of the complex in its ground state (S_0) and in its triplet state (T_1) has been optimized under the density functional level of theory using the PBE1PBE functional, in gas phase and in dichloromethane solution. Figure 4 shows the optimized structures, whereas selected calculated bond lengths and dihedral angles concerning the coordination sphere are given in Table 5.

The ground state (S_0) of [CuI(phen)(py2SH)] adopts a tetrahedral geometry, while a flattening distortion from the tetrahedral geometry by approximately 30 degrees appears in the triplet state (T_1), as expected. In gas phase the triplet state is higher in energy than the singlet state by 1.339eV, while in dichloromethane solution the energy difference between singlet and triplet state is 1.622eV. In the ground state there is an elongation of the Cu_1–I_1 bond in dichloromethane solution compared to gas phase. The other bond distances (Cu_1–N_1, Cu_1–N_2 and Cu_1–S_1) are almost the same in both gas phase and dichloromethane solution. Distortion is also observed in the dihedral angles C_{13}-S_1-Cu_1-N_2 and C_{13}-S_1-Cu_1-N_1 between the gas phase and dichloromethane solution in ground state. A comparison between ground and triplet state, in gas phase, reveals elongation of the Cu_1–I_1 and Cu_1–S_1 bond distances in triplet state, while the Cu_1–N_1 and Cu_1–N_2 bonds are shortened in the excited state in comparison with the singlet state. The same is observed in dichloromethane solution, except from the Cu_1–I_1 bond, which shows a shortening in the triplet state.

gas phase and dichloromethane solution.

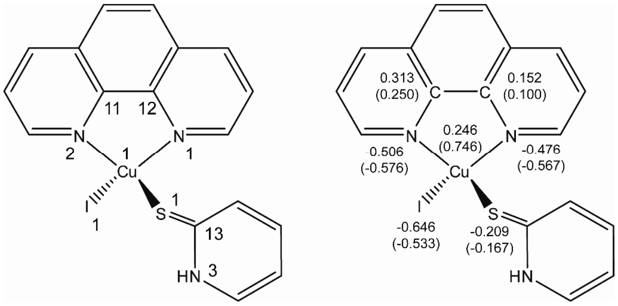

Scheme 2 Skeletal structure of [CuI(phen)(py2SH)] (**3**), studied in this work. (a) The numbering of the main atoms and (b) NBO charges in the singlet (S_0) and triplet (T_1) states (in parentheses). The hydrogen atoms are omitted for sake of clarity

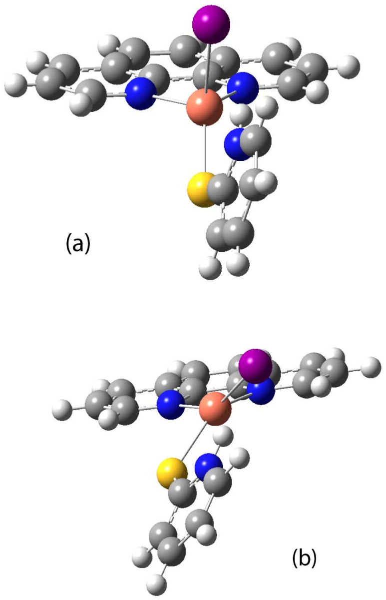

Fig. 4 Optimized geometries of [CuI(phen)(py2SH)] (**3**), for the ground state, S_0, (a) and for the triplet state, T_1, (b) calculated at the PBE1PBE/6-311++G(d,p), SDD level of theory

As it becomes obvious in Scheme 2 (b), the transition of the complex in its lowest triplet excited state is accompanied by an electronic charge displacement from the atoms constituting the chromophore (Cu, S, I) towards the skeleton of the diimine moiety. So, in a first step this leads to an elongation of the bond lengths within the chromophore, which is in accordance to what is observed for the Cu–S and Cu–I bonds. Additionally, the increment of the positive charge of the metal core renders the Cu center to a harder

Dalton Transactions

Dynamic Article Links ►

View Article Online

Cite this: DOI: 10.1039/c0xx00000x

www.rsc.org/xxxxxx

PAPER

Table 5 Relative energies, selected bond distances (Å) and dihedral angles (deg) calculated for complex [CuI(phen)(py2SH)] **(3)** in gas phase and in dichlorometane solution too[a]

	S_0	T_1
Gas Phase		
ΔE (eV)	0.0	1.339
Bond Lengths		
Cu_1-N_1	2.144	1.989
Cu_1-N_2	2.144	1.983
Cu_1-I_1	2.626	2.638
Cu_1-S_1	2.275	2.356
Dihedral Angles		
C_{13}…S_1…Cu_1…N_2	136.5	115.6
C_{13}…S_1…Cu_1…N_1	-136.8	-167.3
N_2…C_{11}…C_{12}…N_1	0.0192	-1.676
CH_2Cl_2 Solution		
ΔE (eV)	0.0	1.622
Bond Lengths		
Cu_1-N_1	2.133	1.993
Cu_1-N_2	2.129	1.977
Cu_1-I_1	2.693	2.656
Cu_1-S_1	2.269	2.329
Dihedral Angles		
C_{13}…S_1…Cu_1…N_2	129.6	108.9
C_{13}…S_1…Cu_1…N_1	-141.0	-171.6
N_2…C_{11}…C_{12}…N_1	0.149	-1.539

[a] Numbering scheme as in Scheme 2a.

Lewis acid and this diminishes its affinity towards the S and I atoms which are typical soft bases, thus contributing further to the elongation of these bonds. On the other hand the increment of the negative charge observed for the N atoms along with atoms C_{11} and C_{12} results in a more negative overall charge located in the chelating region (N_1-C_{11}-C_{12}-N_2) of the phenanthroline ligand. Thus, the higher opposite charges on the metal center and the chelating unit of the phenanthroline ligand when compared to the corresponding ones in the ground state of the system result in a shortening of the Cu–N bond distances in the T_1 state.

The simulated absorption spectrum of CuI(phen)(py2SH)] **(3)**, computed with TD-DFT method at the PBE1PBE/6-311++G(d,p),SDD level of theory on the optimized singlet ground state in dichloromethane solution, is depicted schematically in Figure 5. Selected TD-DFT principal singlet-singlet electronic transitions, excitation energies and oscillator strength in dichloromethane solution are represented in Table 6. The calculated excitation energies are also shown in Figure 6, where representative density diagrams of the MOs participating in each electron transition with the higher CI coefficient are also depicted, in order to intuitively understand the absorption process. The computed electronic transitions are in good agreement with the experimental ones.

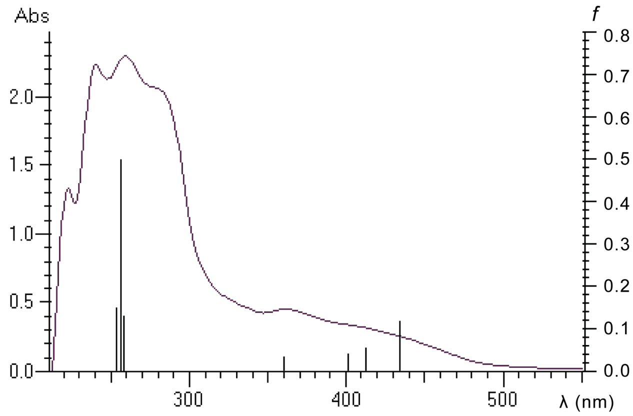

Fig. 5 Experimental absorption spectrum of [CuI(phen)(py2SH)] (**3**) along with the calculated excitation energies appeared as vertical lines.

There is a good resemblance of the calculated excitation energies with the experimental spectra as shown in figure 5. The simulated absorption spectrum shows an intense high energy band in the ultraviolet region (250-300 nm) and a low energy band of lower intensity in the visible region (400-450 nm). The low energy absorption band involves HOMO-1, HOMO-2, HOMO-3 → LUMO excitations and HOMO, HOMO-1→ LUMO+2 excitations. Figure 6 shows that the first three excitations involving MLCT and XLCT transitions, arise from electronic transitions between low energy MOs, which are consisted of Cu 3d AOs, p orbitals located on the iodine ligand and p orbitals located on the sulfur atom of the py2SH ligand, and the high energy LUMO orbital, which is a highly delocalized unoccupied π^*-MO of the phenanthroline.

The second pair of excitations is of the same character (MLCT and XLCT). In particular, the electronic transitions include HOMO and HOMO-1 orbitals, which are consisted of Cu 3d AOs, p orbitals located on the iodine ligand and p AOs of all atoms of py2SH ligand, and the high energy LUMO+2 orbital, which is a highly delocalized unoccupied π^*-MO of the py2SH moiety.

The excitation at 359.8 nm (HOMO-3 → LUMO+1) appears to be of MLCT and XLCT character, considering that it arises from electronic transitions between HOMO-3 orbital, which includes Cu 3d AOs, p orbitals located on iodine ligand and p AOs of all atoms of py2SH ligand, to the high energy LUMO+1 orbital, which is a delocalized unoccupied π^*-MO of the phenanthroline.

Cite this: DOI: 10.1039/c0xx00000x

www.rsc.org/xxxxxx

PAPER

Table 6 Selected principal singlet-singlet transitions in the absorption spectra of complex [CuI(phen)(py2SH)] (**3**), in dichloromethane solution, calculated at the PBE1PBE/6-311++G(d,p)//SDD level of theory

Excitation	E/eV	λ/nm	Orbital Nature	Character	OS, f
HOMO-2→LUMO, HOMO-1→LUMO	2.864	432.9	$3d_{Cu}/\pi_I \rightarrow \pi^*_{phen}$	MLCT/XLCT	0.1212
HOMO-3→LUMO	2.994	414.2	$3d_{Cu}/\pi_I/\pi_{py2SH} \rightarrow \pi^*_{phen}$	MLCT/XLCT	0.0555
HOMO-1→LUMO+2, HOMO→LUMO+2	3.089	401.4	$3d_{Cu}/\pi_I/\pi_{phen} \rightarrow \pi^*_{py2SH}$	MLCT/XLCT	0.0352
HOMO-3→LUMO+1	3.446	359.8	$3d_{Cu}/\pi_I/\pi_{py2SH} \rightarrow \pi^*_{phen}$	MLCT/XLCT	0.0275
HOMO-9→LUMO+1, HOMO-6→LUMO+4	4.803	258.2	$3d_{Cu}/\pi_I/\pi_{py2SH}/\pi_{phen} \rightarrow \pi^*_{phen}$	MLCT/XLCT/IL MLCT/IL	0.1285
HOMO-9→LUMO, HOMO-4→LUMO+3	4.815	257.5	$3d_{Cu}/\pi_I/\pi_{py2SH}/\pi_{phen} \rightarrow \pi^*_{phen}/\pi^*_{py2SH}$	MLCT/XLCT/IL MLCT/IL	0.5045
HOMO-1→LUMO+6	4.885	253.8	$3d_{Cu}/\pi_I \rightarrow \pi^*_{phen}$	MLCT/XLCT	0.1511

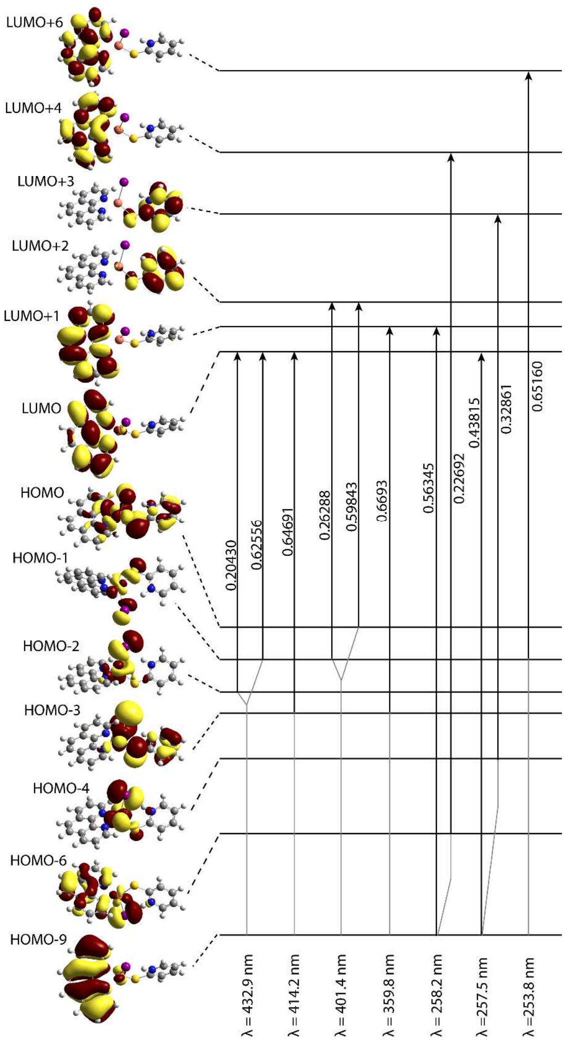

Fig. 6 Excitation energies and single-electron transition with the higher CI coefficient in the TD-DFT calculations for [CuI(phen)(py2SH)] (**3**)

The high energy absorption band involves a series of electronic transitions, the most important of them are referred in Table 5 and depicted in Figure 6. These excitations are also MLCT, XLCT and IL in character and include transitions from occupied orbitals, composed of Cu 3d AOs, p orbitals located on the iodine ligand and p AOs of all atoms of py2SH ligand (at 257.5 and 253.8 nm) or p AOs of the phenanthroline (at 258.2 and 257.5 nm), to high energy unoccupied orbitals, which are consisted of delocalized π^*-MOs of the phenanthroline or py2SH ligands.

Finally, TD-DFT calculations were performed at the PBE1PBE/6-311++G(d,p),SDD level on the optimized first excited triplet state of complex CuI(phen)(py2SH)] **(3)** in dichloromethane solution, in order to calculate the emission spectrum according to the proposed methodology.[55,56] The simulated emission spectrum exhibits a band with a maximum at 514 nm (2.41eV), which is close to the experimentally observed one. The FC-transition from the T_1 state of the complex to its ground state (S_0), resulting to the emission observed is due to a transition from a π-orbital of the diimine ligand to an orbital located on the Cu 3d AOs with a small participation from the pi orbitals of the iodine atom.

4. Conclusions

In this paper we have described the synthesis and characterization of eighteen mixed-ligand copper(I) halide complexes (**1**–**18**), bearing 1,10-phenanthroline and heterocyclic thioamides as ligands. The new compounds formed immediately after mixing of equivalent amounts of the components under mild conditions, are quite instable and their solutions undergo gradual re-colouring from red to green, which indicates oxidation of copper(I) to copper(II). The molecular structures of two representative compounds (**3** and **7**), established by single-crystal X-ray diffraction, feature the metal in a distorted tetrahedral environment surrounded by the two N atoms of the chelating 1,10-phenanthroline, the halogen atom and the thione-S atom of the thioamide. The S-coordination mode of the latter could be verified by the appearance of the four characteristic ‘thioamide bands' in the recorded IR spectra of the complexes. The electronic absorption spectra of these complexes show two main broad bands in the regions 230-260 and 400-430 nm. According to TD-DFT calculations these bands could be assigned as having MLCT/XLCT/IL character. As expected, there is a flattening distortion from the tetrahedral geometry by approximately 30 degrees in the triplet state (T_1) of complex **3** when compared to its ground state (S_0). The $\Delta E_{T_1\text{-}S_0}$ energy gap in the gas phase and in dichloromethane solution is 1.339eV and 1.622eV respectively. Upon $S_0 \rightarrow T_1$ excitation elongation of the Cu–I and Cu–S bond distances is observed, while the Cu–N_1 and Cu–N_2 bonds appear shortened, which is the result of an electronic charge displacement from the atoms constituting the chromophore (Cu, N, S, I) towards the main carbon skeleton of the diimine moiety. An intense emission in the range 490–650 nm is observed for all the complexes under investigation. According to the TD-DFT calculations performed on the optimized first excited triplet state of complex **3** in dichloromethane solution, the emitting excited state consists of π-MOs of the thioamide ligand combined with Cu 3d AOs, p orbitals located on the halide ligand and p orbitals located on the sulfur atom of the thioamide ligand.

Aknowledgements

We thank the EPSRC UK National Crystallographic Service at the University of Southampton for the collection of the crystallographic data.[57]

Notes and References

[a] *Aristotle University of Thessaloniki, Faculty of Chemistry, Inorganic Chemistry Laboratory P.O. Box 135 GR-541 24 Thessaloniki, Greece; E-mail: aslanidi@chem.auth.gr*

[b] *School of Pharmacy and Life Sciences, The Robert Gordon University, Schoolhill, Aberdeen AB10 1FR, Scotland; E-mail: ext.cox1@rgu.ac.uk*

[c] *Aristotle University of Thessaloniki, Faculty of Chemistry, Laboratory of Applied Quantum Chemistry, GR-541 24 Thessaloniki, Greece*

†Electronic Supplementary Information (ESI) available: CCDC-886635 (**3**) and CCDC-886634 (**7**) containing the supplementary crystallographic data for this paper. These data can be obtained free of charge at www.ccdc.cam.ac.uk/conts/retrieving.html [or from the Cambridge Crystallographic Data Centre, 12 Union Road, Cambridge CB2 1EZ, UK; Fax: (intrnat.) + 44-1223/336-033; E-mail: deposit@ccdc.cam.ac.uk]. See DOI: 10.1039/b000000x/

1 B. Minaev, E. Jansson and H. Ågren, *J. Chem. Phys.*, 2006, **125**, 234.
2 B. Minaev, E. Jansson, S. Scrader and H. Ågren, *Chem. Phys.* 2007, **333**, 157.
3 H. Yersin, *Top. Curr. Chem.*, 2004, **241**, 1.
4 C. A. Bignozzi, R. Argazzi and C. J. Kleverlaan, *Chem. Soc. Rev.*, 2000, **29**, 87.
5 D. Felder, J. F. Nierengarten, F. Barigelletti, B. Ventura and N. Armaroli, *J. Am. Chem. Soc*. 2001, **123**, 6291.
6 J. C. Vickery, M. M. Olmstead, E.Y. Fung and A. L. Balch, *Angew. Chem. Int. Ed. Engl.*, 1997, **36**, 1179.
7 M. A. Mansour, W. B. Connick, R. J. Lachicotte, H. J. Gysling and R. Eisenberg, *J. Am. Chem. Soc*., 1998, **120**, 1329.
8 J. N. Demas and B. A. de Graff, *Coord. Chem. Rev*., 2001, **211**, 317.
9 K. E. Erkkila, D. T. Odom and J. K. Barton, *Chem. Rev.*, 1999, **99**, 2777.
10 C. H. Chen and J. Shi, *Coord. Chem. Rev.*, 1998, **171**, 161.
11 C. M. Elliott, F. Pichot, C. J. Bloom and L. S. Rider, *J. Am. Chem. Soc.*, 1998, **120**, 6781.
12 N. Armaroli, *Chem. Soc. Rev*., 2001, **30**, 113, and references therein.
13 D. R. McMillin and K. M. McNett, *Chem. Rev*., 1998, **98**, 1201.
14 D. G. Guttell, S.-M. Kuang, P. E. Fanwick, D. R. McMillin and R. A. Walton, *J. Am. Chem. Soc*., 2002, **124**, 6.
15 S. M. Kuang. D. G. Guttell, D. R. McMillin, P. E. Fanwick and R. A. Walton, *Inorg. Chem.,* 2002, **41**, 3313.
16 L. Yang, J. K. Feng, A. M. Ren, M. Zhang, Y. G. Ma and X. D. Liu, *Eur. J. Inorg. Chem*. 2005, 1867.
17 N. Armaroli, G. Accorsi, M. Holler, O. Moudam, J.-F. Nierengarden, Z. Zhou, R. T. Wegh and R. Welter, *Adv. Mater.*, 2006, **18**, 1313.
18 M. W. Blaskie and D. R. McMillin, *Inorg. Chem.*, 1980, **19**, 3519.
19 C. T. Cunningham, J. J. Moore, K. L. H. Cunningham, P. E. Fanwick and D. R. McMillin, *Inorg. Chem.*, 2000, **39**,3638.
20 D. Felder, J.-F. Nierengarten, F. Barigelletti, B. Ventura and N. Armaroli, *J. Am. Chem. Soc.*, 2001, **123**, 6291.
21 E. S. Raper, *Coord. Chem. Rev*., 1985, **61**, 115.
22 E. S. Raper, *Coord. Chem. Rev*., 1994, **129**, 91.
23 E. S. Raper, *Coord. Chem. Rev*., 1996, **153**, 199.
24 J.A. Garcia-Vazquez, J. Romero and A. Sousa, *Coord. Chem. Rev.*, 1999, **193**, 691.
25 P. Aslanidis, P. J. Cox, K. Kapetangiannis and A. C. Tsipis, *Eur. J. Inorg. Chem*., 2008, 5029.
26 P. Aslanidis, P. J. Cox and A.C. Tsipis, *Dalton Trans*., 2010, **309**, 10238.
27 S. J. Coles and P. A. Gale, *Chem. Sci*., 2012, **3**, 683.
28 Rigaku (2011) *CrystalClear-SM Expert* Rigaku Corporation, Tokio, Japan.
29 G. M. Sheldrick, *Acta Cryst*., 2008, **A64**, 112.
30 A. L. Spek, *Acta Cryst*., 2009, **D65**,148.
31 L. J. Farrugia, *J. Appl. Cryst*., 1979, **32**, 837.
32 M. J. Frisch, G. W. Trucks, H. B. Schlegel, G. E. Scuseria, M. A. Robb, J. R. Cheeseman, J. A. Montgomery, Jr., T. Vreven, K. N. Kudin, J. C. Burant, J. M. Millam, S. S. Iyengar, J. Tomasi, V. Barone, B. Mennucci, M. Cossi, G. Scalmani, N. Rega, G. A. Petersson, H. Nakatsuji, M. Hada, M. Ehara, K. Toyota, R. Fukuda, J. Hasegawa, M. Ishida, T. Nakajima, Y. Honda, O. Kitao, H. Nakai, M. Klene, X. Li, J. E. Knox, H. P. Hratchian, J. B. Cross, C. Adamo, J. Jaramillo, R. Gomperts, R. E. Stratmann, O. Yazyev, A. J. Austin, R. Cammi, C. Pomelli, J. W. Ochterski, P. Y. Ayala, K. Morokuma, G. A. Voth, P. Salvador, J. J. Dannenberg, V. G. Zakrzewski, S. Dapprich, A. D. Daniels, M. C. Strain, O. Farkas, D. K. Malick, A. D. Rabuck, K. Raghavachari, J. B. Foresman, J. V. Ortiz, Q. Cui, A. G. Baboul, S. Clifford, J. Cioslowski, B. B. Stefanov, G. Liu, A. Liashenko, P. Piskorz, I. Komaromi, R. L. Martin, D. J. Fox, T. Keith, M. A. Al-Laham, C. Y. Peng, A. Nanayakkara, M. Challacombe, P. M. W. Gill, B. Johnson, W. Chen, M. W. Wong, C. Gonzalez, and J. A. Pople, Gaussian 03, Revision E.01-SMP, Gaussian, Inc., Pittsburgh PA, 2003.
33 S. Miertus, E. Scrocco and J. Tomasi, *Chem. Phys.*, 1981, **55**, 117.
34 J. Tomasi and M.Persico, *Chem. Rev.*, 1994, **94**, 2027.
35 C. Amovilla, V. Barone, R. Cammi, E. Cancès, M. Cossi, B. Mennucci, C. S. Pomelli and J. Tomasi, *Adv. Quantum Chem.* 1998*,* **32**, 227.
36 J. P. Perdew, K. Burke and M. Ernzerhof, *Phys. Rev. Lett*., 1996, **77**, 3865.
37 J. P. Perdew, K. Burke and M. Ernzerhof, *Phys. Rev. Lett.*, 1997, **78**, 1396.
38 R. Krishnan, J. S. Binkley, R. Seeger and J. A. Pople, *J. Chem. Phys.*, 1980, **72**, 650.
39 A. D. McLean and G. S. Chandler, *J. Chem. Phys*., 1980, **72**, 5639.
40 J-P. Blaudeau, M. P. McGrath, L.A. Curtiss and L. Radom, *J. Chem. Phys*., 1997, **107**, 5016.
41 L. A. Curtiss, M. P. McGrath, J-P. Blandeau, N. E. Davis, R. C. Binning, Jr. and L. Radom, *J. Chem. Phys*., 1995, **103**, 6104.
42 M. N. Glukhovstev, A. Pross, M. P. McGrath and L. Radom, *J. Chem. Phys*., 1995, **103**, 1878.
43 R. M. Everly and D. R. McMillin, *J. Phys. Chem*., 1991, **95**, 9071.
44 W. L. Parker and G. A. Crosby, *J. Phys. Chem*., 1989, **93**, 5692.
45 Q.-H. Jin, X.-L. Xin, C.-J. Dong and H.-J. Zhu, *Acta Cryst*., 1998, C**54**, 1097.
46 X.-P. Zhou, D. Li and S. W. Ng, *Acta Cryst*., 2005, E**61**, m654.
47 Y.-L. Xiao, L.-L. Zhou, S. Gao, Q.-H. Jin and C.-L. Zhang, *Acta Cryst*., 2011, E**67**, m1713.
48 J. Nie, J. Wang and C. Dai, *Acta Cryst*., 2010, E**66**, m1538.
49 Q. Meng, Y. Chen, B. Li, S. Chen and S. Gao, *Acta Cryst*. 2011, E**67**, m226.

50 S. Divanidis, P. J. Cox, P. Karagiannidis and P. Aslanidis, *Polyhedron*, 2005, **24**, 351.
51 P. J. Cox, A. Kaltzoglou and P. Aslanidis, *Inorg. Chim. Acta*, 2006, **359**, 3183.
52 P. Karagiannidis, S. K. Hadjikakou, P. Aslanidis and A. Hountas, *Inorg. Chim. Acta*, 1990, **178**, 27.
53 M. Forward, D. Bohmann, J. P. Fackler Jr. and R. J. Staples, *Inorg. Chem.*, 1995, **34**, 6330.
54 H. Araki, K. Tsuge, Y. Sasaki, S. Ishizaka and N. Kitamura, *Inorg Chem***.,** 2005**, 44**, 9667.
55 D. Jacquemin, E. A. Perp`ete, G. Scalmani, M. J. Frisch, I. Ciofini and C. Adamo, *Chem. Phys. Lett*., 2006, **421**, 272.
56 D. Jacquemin, E. A. Perp`ete, X. Assfeld, G. Scalmani, M. J. Frisch and C. Adamo, *Chem. Phys. Lett.*, 2007*,* **438**, 208.
57 S. J. Coles and P. A. Gale, *Chem. Sci.*, 2012, **3(3)**, 683.